International Journal of Mechanical, Industrial and Aerospace Sciences
ISSN: 2517-9950
Vol:4, No:2, 2010

Influence of Outer Corner Radius in Equal Channel Angular Pressing

Basavaraj V. Patil[1], Uday Chakkingal[2] and T. S. Prasanna Kumar[2]

***Abstract*—**Equal Channel Angular Pressing (ECAP) is currently being widely investigated because of its potential to produce ultra-fine grained microstructures in metals and alloys. A sound knowledge of the plastic deformation and strain distribution is necessary for understanding the relationships between strain inhomogeneity and die geometry. Considerable research has been reported on finite element analysis of this process, assuming three-dimensional plane strain condition. However, the two-dimensional models are not suitable due to the geometry of the dies, especially in cylindrical ones. In the present work, three-dimensional simulation of ECAP process was carried out for six outer corner radii (sharp to 10 mm in steps of 2 mm), with channel angle 105°, for strain hardening aluminium alloy (AA 6101) using ABAQUS/Standard software. Strain inhomogeneity is presented and discussed for all cases. Pattern of strain variation along selected radial lines in the body of the work-piece is presented. It is found from the results that the outer corner has a significant influence on the strain distribution in the body of work-piece. Based on inhomogeneity and average strain criteria, there is an optimum outer corner radius.

***Keywords*—** Equal Channel Angular Pressing, Finite Element Analysis, strain inhomogeneity, plastic equivalent strain, ultra fine grain size, aluminium alloy 6101.

I. Introduction

ULTRA-FINE grained materials have been widely investigated due to their improved mechanical properties such as high strength and ductility. Various techniques have been developed to obtain such mechanical properties. Among these, the Equal Channel Angular Pressing (ECAP), originally developed by V. M. Segal [1-2], is one of the effective methods of obtaining materials with high strength and toughness. In ECAP, a work-piece is pressed through a die that contains two channels with equal cross-section meeting at an angle 2ϕ, having corner angle ψ and outer corner radius R as shown in Fig. 1. Since the cross-section of the work-piece remains unchanged, the process can be repeated until the accumulated deformation reaches a desired level. High strain can be achieved with multiple passes due to its cumulative nature. In multiple pass, different routes may be employed; Route A: in which the orientation of work-piece remains unchanged in successive passes; Route B: in which the work-piece is rotated by 90° about its longitudinal axis; Route C: in which the work-piece is rotated by 180° about its longitudinal axis.

[1] Ph.D.; Department of Industrial & Production Engineering, BVB College of Engineering & Technology, Hubli-580031 (India);
Email: patilbv@gmail.com; Phone: 00919379662424
[2] Ph.D.; Department of Metallurgical & Materials Engineering, Indian Institute of Technology – Madras, Chennai-600036 (India).

The work-piece under extrusion can be divided into four zones namely (a) head (the front of the work-piece), (b) body, (c) plastic deformation zone and (d) tail (the undeformed portion at the end of the work-piece) as shown in Fig. 2. It is important to know the effect of geometry on the distribution of strain in these zones. The strain per pass can be calculated by the equation (developed by Iwahashi [3])

$$\bar{\varepsilon}_p = \frac{1}{\sqrt{3}}\left[2\cot\left(\phi+\frac{\psi}{2}\right)+\psi\cos ec\left(\phi+\frac{\psi}{2}\right)\right] \quad (1)$$

where $\bar{\varepsilon}_p$ is the equivalent plastic strain (termed as 'strain' for convenience in this paper), 2ϕ is the channel angle and ψ is the corner angle as shown in Fig. 1. It is a closed equation with two parameters (ψ and 2ϕ), that predicts $\bar{\varepsilon}_p$ for a given die geometry. The strain obtained from the equation does not give details of strain variation across the cross section of the work-piece. The distribution of strain is greatly influenced by the outer corner radius and this can be obtained by Finite Element Method.

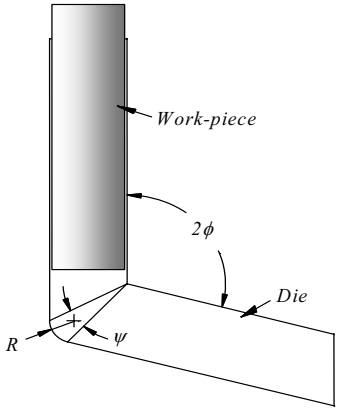

Fig. 1: Schematic of ECAP

Finite element method is one of the important approaches to understand the deformation occurring in the ECAP process. Many FEM-based analyses have been performed to determine the deformation behavior of materials and to estimate the developed strain in the ECAP process. These include the effect of friction on material flow [4], the influence of material model [5], the effect of back pressure on the strain [6], the effect of the channel angle on the deformation of work-piece and the dependence of the strain achieved in the work-piece

on parameters like coefficient of friction, corner radius etc. [7-13]. Yoon *et. al* [14] presented effect of outer corner radius and strain hardening exponent. All these works are based on assumption of two-dimensional plane-strain condition. Recently three-dimensional models have been used for the analysis [15 - 18] but no extensive work has been reported.

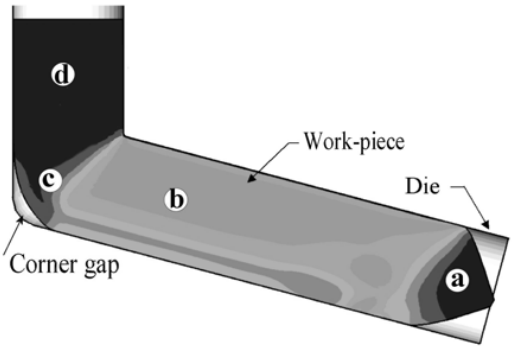

Fig. 2: Different zones of deforming work-piece (a) head (b) body (c) plastic deformation zone (d) tail

In the present study, a three-dimensional deformation analysis was carried out for six outer corners, sharp to 10 mm, in steps of 2 mm, with channel angle of 105°. The motivation was to understand the influence of the outer corner radius on material flow and strain inhomogeneity. The general-purpose finite element software ABAQUS/Standard, which has the capability to model non-linear stress analysis accurately and reliably [19], was used. The influence of outer corner radius on the distribution of strain in the important zones for all radii is presented and discussed.

To understand the pattern of strain variation, five radial lines, separated by 45° were chosen for study as shown in Fig. 3. The line from the center of the work-piece to the upper surface was denoted as Line-1 and to the lower surface was denoted as Line-5. Variation of strain along these lines is presented and discussed. In addition to the variation of strain along the radial lines, average strain and strain inhomogeneity across different sections in the body of the work-piece are presented and discussed.

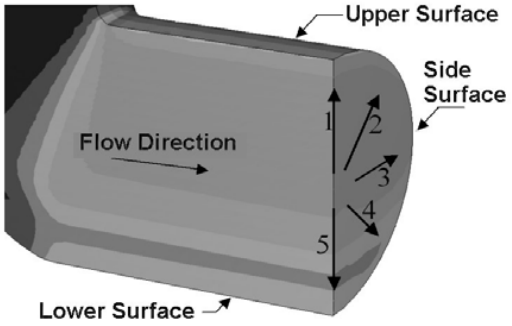

Fig. 3: Radial lines considered for study

II. Finite Element Simulation

In the present work, a three-dimensional model was considered for analysis to understand the influence of outer corner of the die on strain distribution. Two dimensional plane strain approximation can be used when the thickness of the work-piece is very large and plane stress approximation can be used when the thickness is very small. Both the plane strain and plane stress conditions are not applicable for the round work-piece used in ECAP. Axi-symmetric approximation is not suitable because the axis of the channels intersect at an angle 2ϕ . Results obtained by two-dimensional analysis give limited information in addition to the inherent two-dimensional approximation errors. three-dimensional analysis gives clear idea of strain in different zones at different sections.

A cylindrical work-piece of diameter 20 mm and length 105 mm, made of aluminum alloy was used. At the front side, filleting of 1 mm x 1 mm was done. Only half portion of work-piece and die was considered for modeling because of the symmetry about the parting surface. Material used for work-piece was Aluminum alloy AA 6101 with flow stress given by $\sigma_0 = 208\varepsilon^{0.25}$, obtained experimentally [21] using compression test. A Yield stress of 75.8 MPa, Poisson's ratio of 0.33 and Young's modulus of 69 GPa were assumed. The work-piece was modeled with 7600 nodes and 6320 elements using 8 node linear hexahedral elements (C3D8)[19]. The stress-strain curve used for analysis is shown in Fig. 4. It was assumed that the hardening behavior was isotropic and independent of strain rate at room temperature. Heat generated due to deformation and friction was neglected. The coefficient of friction was assumed to be 0.1, which was a reasonable value for cold forming condition.

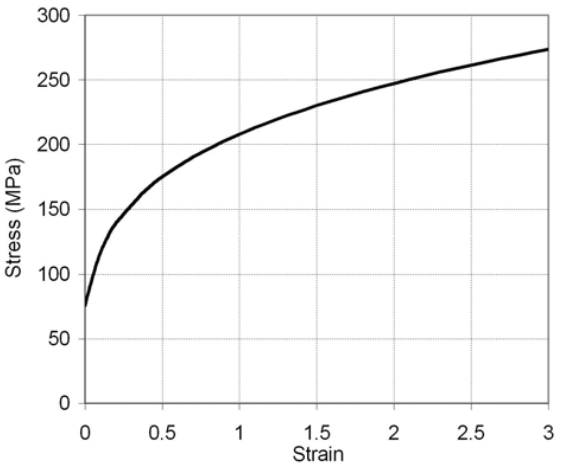

Fig. 4: Stress-Strain curve of AA6101 Aluminum

The die considered for analysis was made of high strength steel. As the strength and rigidity of steel die were very high compared to aluminium, the die was modeled as rigid surface with linear quadrilateral elements (R3D4)[19]. Because of the

symmetry only half portion was considered for analysis as shown Fig. 5. Six different conditions were considered to model the die with channel angle 105° for different outer corners, namely, sharp, 2 mm, 4 mm, 6 mm, 8 mm and 10 mm, denoted as R00, R02, R04, R06, R08, and R10 respectively. Numbers of elements and nodes used varied between 2300 and 2700, depending on the outer radius of the die.

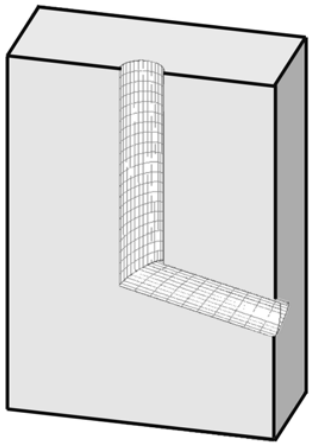

Fig. 5. Die and the internal surface used for meshing

The boundary conditions applied to the model were as listed below:

- Displacement and rotation in x, y and z direction for all nodes in the die were arrested.
- As the conditions were symmetric about the parting plane of the work-piece, only half portion was modeled and all the nodes of the work-piece on this plane were given symmetry condition. The symmetry boundary condition arrests the displacement in the direction perpendicular to the plane and rotation about other two directions.
- The top surface of the work-piece was in contact with the punch resulting in the movement of the work-piece. Hence, all nodes on the top surface of the work-piece were given displacement in the direction of movement of the punch.

A. Average equivalent plastic strain:

The average equivalent plastic strain in the body of the work-piece was obtained by

$$Avg\bar{\varepsilon}_p = \frac{1}{n}\sum_{i=1}^{n}\bar{\varepsilon}_p^i \tag{2}$$

where n is number of nodes in the body of the work-piece and $\bar{\varepsilon}_p^i$ is equivalent plastic strain at the node i.

B. Quantification of Strain Inhomogeneity

In the literature [5, 17 and 20] inhomogeneity is expressed as an index (C_i), which is defined as

$$C_i = \frac{Max\bar{\varepsilon}_p - Min\bar{\varepsilon}_p}{Avg\bar{\varepsilon}_p} \tag{3}$$

where $Max\bar{\varepsilon}_p$, $Min\bar{\varepsilon}_p$, and $Avg\bar{\varepsilon}_p$ are maximum, minimum and average equivalent plastic strains respectively. In defining inhomogeneity in this form only the difference between two extreme values of the strain is used. It does not take into account the distribution of strain. Hence in this work, a more appropriate way of quantifying the strain inhomogeneity is adopted, given by coefficient of variance of strain ($CV\bar{\varepsilon}_p$), defined as

$$CV\bar{\varepsilon}_p = \frac{Stdev\bar{\varepsilon}_p}{Avg\bar{\varepsilon}_p} \tag{4}$$

where $Stdev\bar{\varepsilon}_p$ is the standard deviation of equivalent plastic strain [22]. The inhomogeneity defined in the form of $CV\bar{\varepsilon}_p$ is a better measure as it uses standard deviation, which is based on distribution of strain in the entire domain. In case of ideal homogeneity both C_i and $CV\bar{\varepsilon}_p$ will have the value of zero.

III. Results and Discussion

Based on the results obtained from the simulation, the influence of the outer corner on plastic deformation zone, the strain distribution in the body and the strain variation along the selected radial lines are discussed in this section. This will help to understand and correlate the distribution of strain, microstructure and other material properties in the ECAP process.

A. Influence on the plastic deformation zone:

The plastic deformation zone was found to be narrow for sharp corner dies. As corner radius increased, the plastic deformation zone widened and covered the corner angle ψ as show in the Fig. 6(a-f).

B. Influence on strain distribution over the work-piece body:

The Iwahashi strain obtained by Eqn.1 and the simulated average strain obtained by Eqn.2 for the body of the work-piece are shown in the Fig. 7. The trend was linear with the average strain reducing with the increasing outer corner radius. However there was a difference of 6% between Iwahashi strain and simulated strain mainly due to the complicated geometry at the intersection of cylindrical channel, unlike rectangular channel assumed by Iwahashi and, secondly, the presence of initial corner gap.

The coefficient of variance of strain $CV\bar{\varepsilon}_p$ obtained using the Eqn. 4 for different outer corners is shown in Fig. 8. The figure shows the influence of outer corner radius on the inhomogeneity with an optimal value around 4 mm for the cases studied. In case of sharp and small outer corner dies, high strain is developed during deformation at the outer corner and is more than the average strain. In case of larger outer

corner dies, the strain developed during deformation at the outer corner is lower than the average strain. Therefore both small and large outer corner dies result in higher inhomogeneity while an intermediate outer corner results in minimum inhomogeneity. For the material and working conditions assumed the optimum outer corner radius was found to be 4 mm.

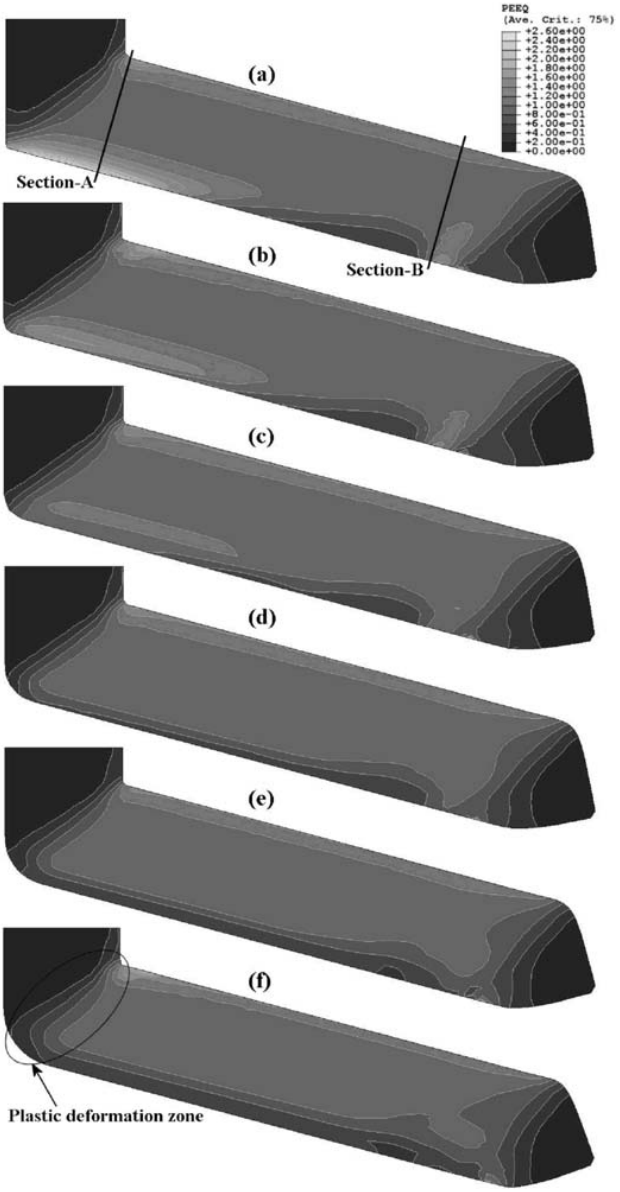

Fig. 6: Equivalent plastic strain along the longitudinal section (a) Sharp (b) 2 mm (c) 4 mm (d) 6 mm (e) 8 mm (f) 10 mm outer corner

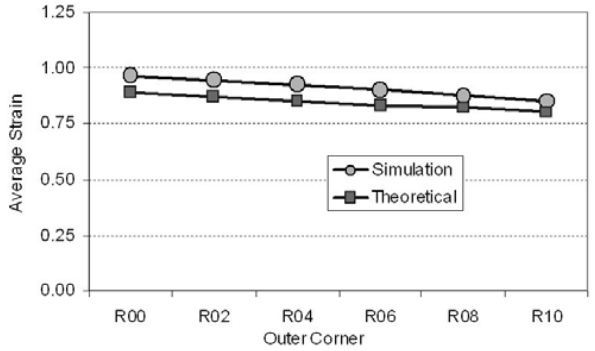

Fig. 7: Average equivalent plastic stain in body of the work-piece and Iwahashi strain

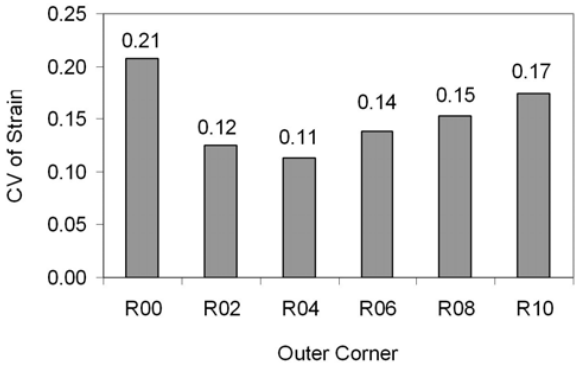

Fig. 8: Coefficient of Variance of strain in the body of the work-piece

C. Influence on strain distribution along the work-piece axis:

Inhomogeneity exists along the axis of the work-piece also. To study this, forty sections along the axis of the work-piece (numbered 1 to 40 between sections A and B as shown in Fig. 6(a)) were considered. Section A was 80 mm and section B was 25 mm away form the leading point of the head, enclosing the useful portion of the work-piece.

The strain inhomogeneity at the sections considered is shown in Fig. 9. The variation in strain inhomogeneity was very high for the dies with sharp and 2 mm corner. For all other dies the strain inhomogeneity increased towards the head (towards section B - Fig. 9). This can be attributed to variation in the opposing frictional force in the exit channel and the presence of an initial corner gap. Formation of an initial corner gap was observed for all cases. As the process continued backpressure developed and the corner gap started filling. For larger outer corners, the corner gap was filled quickly and there was no further change in geometrical parameters resulting a constant strain inhomogeneity. For sharp and smaller corners it took more time to fill the corner gap with continuous change in the geometrical parameters resulting in a large variation in strain inhomogeneity.

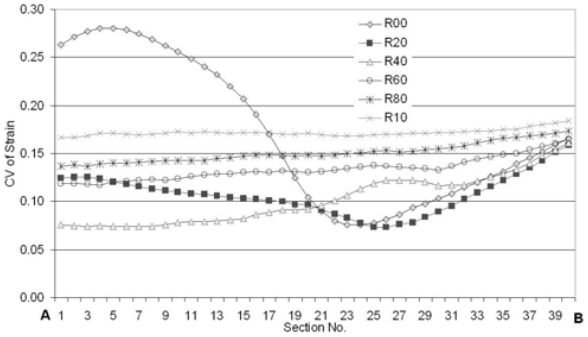

Fig. 9: Coefficient of Variance of strain at different sections in the body of the work-piece

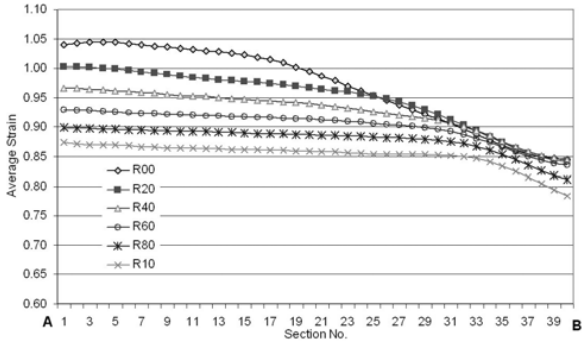

Fig. 10: Average strain at different sections in the body of the work-piece

The average strain at different sections along the axis of work-piece body is show in Fig. 10. For all cases the average strain decreased towards the head, which can be attributed to presence of initial corner gap and it's filling due to backpressure as explained above.

D. Influence on strain distribution along radial lines:

Figure 11(a-f) shows the distribution of strain across the work-piece body at section-A for different outer corners. There was a gradual change in the strain distribution from one section to another. Figure 12(a-f) shows the variation of strain averaged between sections A and B along the radial lines. It indicates that the influence of outer corner radius on the strain distribution along the radial lines is significant.

- Along the lines from the center to the upper surface (Line-1 and Line-2) strain remained constant up to 80% of the radius and increased near the surface for all cases. The increase in strain near the upper surface was due to deformation at the sharp inner corner. There was no influence of outer corner radius on the strain distribution along these lines.
- Strain remained constant along the line from the center to the side surface (Line-3) and was not influenced by outer corner for all cases.
- Along the lines from the center to the lower surface (Line-4 and Line-5) the strain remained constant up to 50% of the radius. Further the strain decreased for larger outer corners but decreased for sharp and 2 mm corner radius dies. The influence of outer corner radius was very high on the strain distribution along these lines.

In general from the center up to 50% of the radius the strain was more or less constant, which implies that the contribution to the strain inhomogeneity from the core is lesser than the remaining outer region.

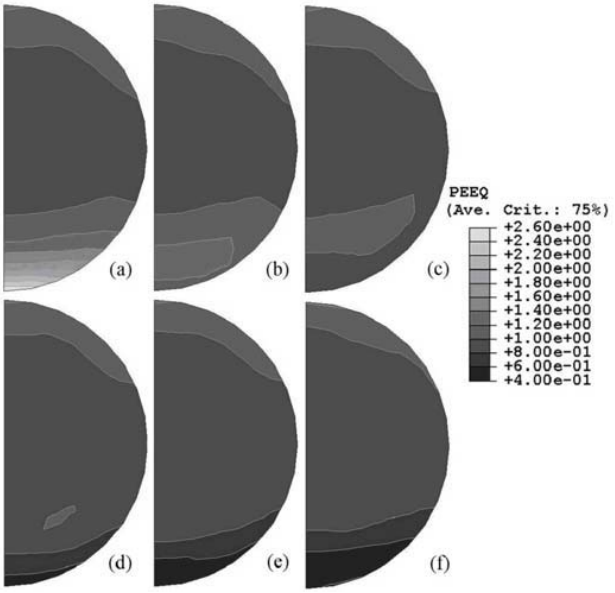

Fig. 11: Equivalent plastic strain across the Section-A in the work-piece body (a) Sharp (b) 2 mm (c) 4 mm (d) 6 mm (e) 8 mm (f) 10 mm outer corner

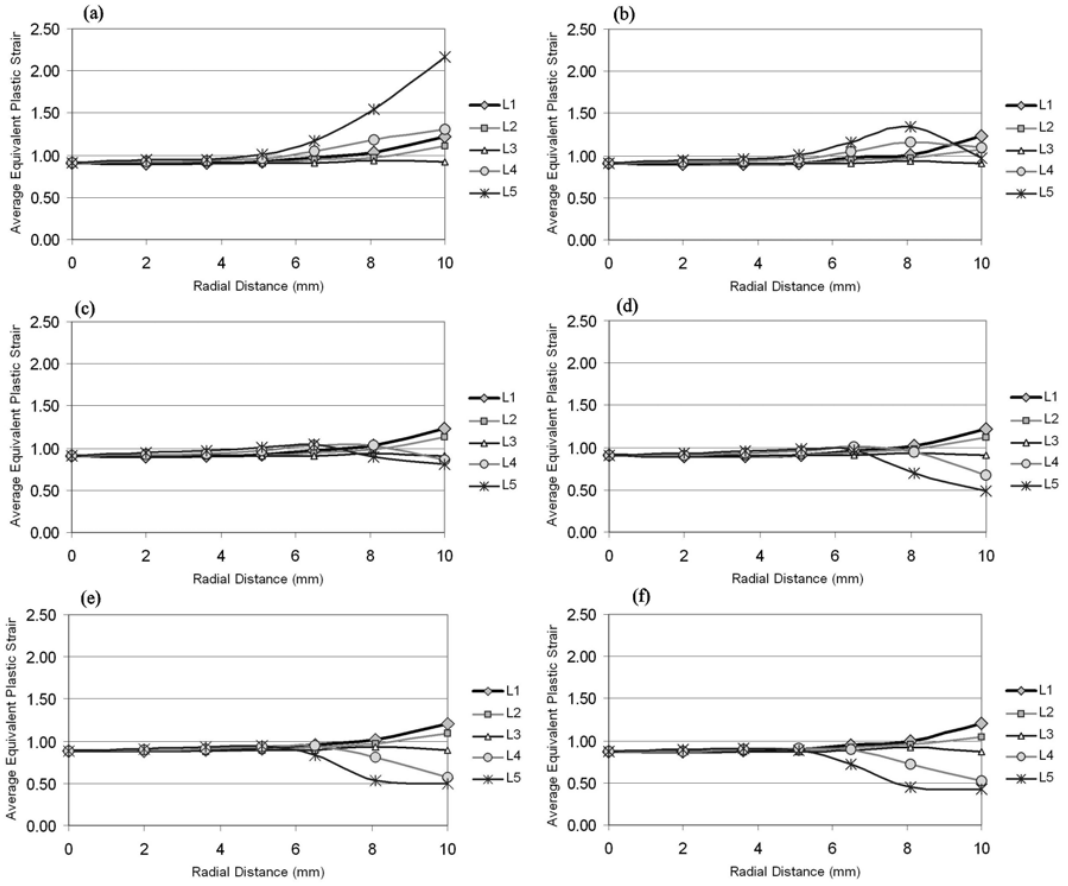

Fig. 12: Equivalent plastic strain (averaged over the body between section A and B) along the radial lines

IV. Conclusion

Three-dimensional finite element analysis was carried out for different outer corner radii in equal channel angular pressing with 105° channel angle. Isotropic strain hardening aluminium alloy AA6101 was chosen as material.

The study revealed the following:

- The radius of outer corner of the die had an important role on strain (equivalent plastic strain $\bar{\varepsilon}_p$) distribution in the work-piece.
- The average strain decreased from 0.97 to 0.85 as the outer corner radius was increased from zero (sharp) to 10 mm.
- Strain inhomogeneity was found to be high for both sharp and large outer corner dies, with a minimum in between which could be regarded as optimal shape for outer corner. Such an optimal outer corner was found to be 4 mm for the cases studied.
- The average strain was found to decrease towards the head of the work-piece for all cases.
- Strain was more or less uniform for about half the diameter of work-piece (inner core) while the strain distribution was found to be quite significant in the periphery, extending to about half the thickness of the work-piece.

References

[1] V. M. Segal, "Material Processing by simple shear", Mater. Sci. Eng. A 197 (1995) 157-164.
[2] V. M. Segal, "Equal channel angular extrusion: from macromechanics to structure formation", Mater. Sci. Eng. A 271 (1999) 322-333.
[3] Y. Iwahashi, J. Wang, Z. Horita, M. Nemoto, T. G. Langdon, "Principles of equal channel angular pressing of ultra-fine grained materials", Scripta Mater. 35 (2) (1996) 143.
[4] Yi-Lang, Shyong Lee, "Finite element analysis of strain conditions after equal channel angular extrusion", J. Mater. Tech. 140 (2003) 583-587.
[5] S. Li, M. A. M. Bourke, I. J. Beyerlein, D. J. Alexander, B. Clausen, "Finite element analysis of the plastic deformation zone and working load in equal channel angular extrusion", J. Mater. Eng. A 382 (2004) 217-236.
[6] Hl-Heon Son, Jeong-Ho Lee, Yong-Taek Im, "Finite element investigation of equal channel angular extrusion with back pressure", J. Mater. Process. Technol. 171 (2006) 480-487.
[7] C. J. Luis-Perez, R. Luri-Irigoyen, D. Gaston-Ochao, "Finite element modeling of an Al-Mn alloy by equal channel angular extrusion", J. Mater. Process. Tech. 153-154 (2004) 846-852.
[8] Raghavan Srinivasan, "Computer simulation of the equal channel angular extrusion (ECAE) process", Scripta Mater. 44 (2001) 91–96.
[9] H. S. Kim, "Finite element analysis of equal channel angular pressing using a round corner die", Mater. Sci. Eng. A 315 (2001) 122–128.
[10] A. V. Nagasekhar and Yip Tick-Hon, "Optimal tool angles for equal channel angular extrusion of strain hardening materials by finite element analysis", Comp. Mater. Sci. 30(3-4) (2004) 489-495
[11] H. S. Kim, M. H. Seo and S. I. Hong, "Finite element analysis of equal channel angular pressing of strain rate sensitive metals", J. Mater. Process. Tech. 130–131 (2002) 497–503.

[12] A. V. Nagasekhar, Y. Tick-Hon, S. Li and H. P. Seow, "Effect of acute tool-angles on equal channel angular extrusion/pressing", Mater. Sci. Eng. A 410-411 (2005) 269-272.
[13] Fuqian Yang, Aditi Saran, K. Okazaki, "Finite element simulation of equal channel angular extrusion", J. Mater. Process. Tech. 166 (2005) 71-78.
[14] S. C. Yoon, P. Quang, S. I. Hong, H. S. Kim, "Die design for homogeneous plastic deformation during equal channel angular pressing", J. Mater. Process. Tech. 187-188 (2007) 46-50
[15] C. W. Su, L. Lu and M. O. Lai, "3D finite element analysis on strain uniformity during ECAP process", Mater. Sci. Tech. 23-6 (2007) 27-735.
[16] Hong Jiang, Zhiguo Fan, Chaoying Xie, "3D finite element simulation of deformation behavior of CP-Ti and working load during multi-pass equal channel angular extrusion", Mater. Sci. Eng. A (2007).
[17] Tao Suo, Yulong Li, Qiong Deng, "Yuanyong Liu, Optimal pressing route for continued equal channel angular pressing by finite element analysis", Mater. Sci. Eng. A 466 (2007) 166-171.
[18] J. K. Kim, W. J. Kim, "Analysis of deformation behavior in 3D during equal channel angular extrusion", J. Mater. Process. Tech. 176 (2006) 260-267.
[19] ABAQUS User's Manual, Version 6.5.1, Hibbitt, Karisson & Sorensen 2006.
[20] C. Xu, K. Xia and T. G. Langdon, "The role of back pressure in the processing of pure aluminum by equal-channel angular pressing", Acta Mater., 55 (2007) 2351–2360
[21] D. Nagarajan, "Processing of an aluminium alloy by ECAE prior to cold extrusion", M.S. Thesis, Indian Institute of Technology Madras, India, 2005, 47.
[22] Patil Basavaraj V. Uday Chakkingal, T.S. Prasanna Kumar, "Study of channel angle influence on material flow and strain inhomogeneity in equal channel angular pressing using 3D finite element simulation", Jl. of Mater. Process. Tech. 209 (2009) 89-95.